Research Article

Received: 19 May 2022 Revised: 31 August 2022 Accepted article published: 11 September 2022 Published online in Wiley Online Library: 26 September 2022

(wileyonlinelibrary.com) DOI 10.1002/jsfa.12221

Emodin modulates gut microbial community and triggers intestinal immunity

Humphrey A. Mabwi,[a,b,c,d†] Hee Ju Lee,[a†] Emmanuel Hitayezu,[a] Intan Rizki Mauliasari,[a] Cheol-Ho Pan,[a,d] Kilaza Samson Mwaikono,[e] Erick V. G. Komba,[c] Choong-Gu Lee[a,d*] and Kwang Hyun Cha[a*]

Abstract

BACKGROUND: The gut microbiota (GM) plays an important role in human health and is being investigated as a possible target for new therapies. Although there are many studies showing that emodin can improve host health, emodin–GM studies are scarce. Here, the effects of emodin on the GM were investigated *in vitro* and *in vivo*.

RESULTS: *In vitro* single bacteria cultivation showed that emodin stimulated the growth of beneficial bacteria *Akkermansia*, *Clostridium*, *Roseburia*, and *Ruminococcus* but inhibited major gut enterotypes (*Bacteroides* and *Prevotella*). Microbial community analysis from a synthetic gut microbiome model through co-culture indicated the consistent GM change by emodin. Interestingly, emodin stimulated *Clostridium* and *Ruminococcus* (which are related to *Roseburia* and *Faecalibacterium*) in a mice experiment and induced anti-inflammatory immune cells, which may correlate with its impact on specific gut bacteria.

CONCLUSION: Emodin (i) showed similar GM changes in monoculture, co-culture, and in an *in vivo* mice experiment and (ii) simulated regulatory T-cell immune responses *in vivo*. This suggest that emodin may be used to modulate the GM and improve health.

Supporting information may be found in the online version of this article.

Keywords: emodin; gut microbiome; MiSeq; T regulatory cell

INTRODUCTION

Anthraquinone-containing plants, such as rhubarb and aloe, have been used as phytomedicines for over 4000 years.[1] Emodin is the main anthraquinone in rhubarb and possesses a wide spectrum of pharmacological activities, including antimicrobial, antidiabetic, immunosuppressive, neuroprotective, and hepatoprotective activities.[2] Despite its positive pharmacological effects, emodin has shown extremely low oral bioavailability in rats (3%) due to significant glucuronidation, which limits its clinical applicability.[3] Nevertheless, most phytomedicines are administered orally and exert their biological effects after interacting with the gut microbiota (GM).[4] Hence, the GM may play a vital role in the metabolism and efficacy of orally administered emodin.

GMs are critical for maintaining intestinal homeostasis and the host's health.[5] GM dysregulation is linked to diverse disorders, such as gastrointestinal inflammatory disorders associated with dysbiosis[6] and compromised immunosuppressive functions of forkhead box P3 transcription factor 3 (Foxp3) + T regulatory (Treg) cells.[7] Previous results indicated that the induction and maintenance of colonic Treg cells critically depend on the GM.[8] Therefore, the GM has also been implicated in host immunity by potentiating the generation of anti-inflammatory Treg cell populations.[9] Treg cells comprise a subset of cluster of differentiation 4

* *Correspondence to: KH Cha or C-G Lee, Natural Product Informatics Research Center, Korea Institute of Science and Technology, Gangneung 25451, South Korea. E-mail: chakh79@kist.re.kr (Cha); E-mail: cglee0708@kist.re.kr (Lee)*

† *These authors contributed equally to this work.*

a *Natural Product Informatics Research Center, Korea Institute of Science and Technology, Gangneung, South Korea*

b *Department of Microbiology, Parasitology, and Biotechnology, College of Veterinary Medicine and Biomedical Sciences, Sokoine University of Agriculture, Morogoro, Tanzania*

c *SACIDS Foundation for One Health, College of Veterinary Medicine and Biomedical Sciences, Sokoine University of Agriculture, Morogoro, Tanzania*

d *Division of Bio-Medical Science and Technology, KIST School, University of Science and Technology, Seoul, South Korea*

e *Department of Science and Laboratory Technology, Dar es Salaam Institute of Technology, Dar es Salaam, Tanzania*

(CD4) + T cells with suppressive functions and are characterized by expression of the transcription factor Foxp3.[10] Consequently, numerous methods have been developed to regulate the GM composition and, thus, its metabolic and immunological activities, such as the use of probiotics, prebiotics, and phytochemicals.[11]

Previous studies on GM and phytochemical interactions have mostly involved culturing single bacterial cultures with the chemical of interest,[12] culturing entire fecal-material samples,[4] or *in vivo* animal models to study the effects of the GM directly.[13] However, the GM is composed of several co-existing microorganisms, and monocultures treated with phytochemicals of interest could insufficiently represent the natural interactions within the GM community.[14] However, culturing fecal samples with chemicals of interest may fail to adequately screen the GM for interactions with phytochemicals, as it contains many microbial species that vary between people.[15] In this regard, it could be appropriate to study synthetic GM communities as a bottom-up approach for co-culturing gut bacteria with phytochemicals while simulating the mucosal environment.[16]

Despite the benefits of emodin on GM interactions in alleviating kidney-related diseases and more recently in counteracting iodine-induced thyroiditis, previous studies on emodin–GM interactions are still scarce.[17,18] In this study, we tried to determine whether emodin can actually change the gut microbial community through *in vitro* bacteria cultivation. Additionally, through *in vivo* experiments, it was investigated whether the interaction between emodin and GM was related to the changes in physiological activity in experimental mice. We also examined the change in intestinal Treg immunity in emodin-administered mice to evaluate the role of the gut microbiome modulation by emodin in host immunity.

MATERIALS AND METHODS

Preparing bacteria and chemical compound stocks

To mirror human GM species, human GM isolates that are abundant in the human gut[19] were obtained from Korean Collection for Type Cultures (KCTC, Daejeon, Korea) and American Type Culture Collection (Rockville, MD, USA) (Supporting Information Table S1). Isolates were recovered as recommended by the Korean Collection for Type Cultures and American Type Culture Collection. Briefly, bacteria were first cultured in the respective recommended medium (Supporting Information Table S1) at 37 °C under anaerobic conditions for 18–24 h. Then, each bacterial culture was mixed with sterilized and deoxygenized glycerol (50%) and stored at −80 °C for subsequent analyses. All chemicals were purchased from Sigma-Aldrich (St. Louis, MO, USA) and dissolved in pure dimethyl sulfoxide (DMSO) to obtain stock concentrations of 10 mmol L^{-1} used in our *in vitro* study.

For our *in vitro* study, chemical treatment was performed using Gifu anaerobic medium (GAM). This medium is recommended as a general culture medium for cultivating and isolating anaerobic bacteria.[20] Additionally, GAM does not require supplementation with horse blood, which enables it to remain transparent after autoclaving for easier growth monitoring at an optical density of 600 nm ($OD_{600\ nm}$). The compositions of GAM are as shown in Supporting Information Table S2.

Monocultures with chemical compounds

Bacterial strains were grown twice for 18–24 h to obtain a robust and uniformly growing culture before inoculating the screening plates. The optical density of each overnight pre-culture was measured and subsequently diluted to a desired screening $OD_{600\ nm}$ of 0.1. Next, 2% of this diluted inoculum was added to a fresh GAM, and 1800 µL was dispensed into 96-well, deep-well plates followed by chemical treatment at a final concentration of 100 µmol L^{-1}. Next, 200 µL of this volume (1800 µL) was dispensed into 96-well screening plates. To study the potential toxicity of using DMSO as the solvent, the same bacterial volume was incubated with medium containing DMSO (1%), without added chemicals. 'Single-blank medium' solutions, comprising a chemical compound of interest alone, were included to assess the influence of each chemical compound on the optical density measurement. 'Double-blank medium' solutions, without bacteria or the chemical compound of interest, were used as a negative control to determine whether the 18–24 h incubation at 37 °C influenced the medium turbidity. The values obtained for the blank samples were subtracted from the sample-turbidity values. The results obtained were expressed as a percentage of the positive control (DMSO only) in a heatmap to facilitate the comparison between different chemical compounds used in this experiment. After inoculation, the plates were incubated at 37 °C in an anaerobic chamber, without shaking.

Growth was determined by tracking the endpoint absorbance at $OD_{600\ nm}$ after 18–24 h of incubation ($n = 8$ per bacteria) using a Synergy HT microplate reader (BioTek Instruments, Winooski, VT, USA) with low-speed shaking for 5's before each reading. All media were pre-reduced at least 1 day before use under anoxic conditions in an anaerobic chamber (Coy Laboratory Products Inc., Grass Lake, MI, USA) (2% hydrogen, 12% carbon dioxide, 86% nitrogen), and all experiments were performed under anaerobic conditions at 37 °C, unless specified otherwise. Bacteriological media were acquired from MB Cell (Seoul, South Korea), and other chemicals were acquired from Sigma-Aldrich unless stated otherwise.

Synthetic gut microbial consortium reconstruction and emodin treatment

Synthetic gut microbial communities were cultured in tubes designed to represent both the mucosal and luminal microbiota. For this purpose, mucin–agar gel was used to simulate the mucosal environment, as previously described.[16] Briefly, the mucin–agar gel was prepared using a combination of porcine type-III gastric mucin and agar at a 50 g L^{-1}:30 g L^{-1} ratio. The pH was adjusted to 6.5 with 1 mol L^{-1} hydrochloric acid before autoclaving. After autoclaving, approximately 2 mL of mucin–agar was pipetted into different 14 mL culture tubes and allowed to solidify in an anaerobic chamber. Single-use bacterial stocks in 50% glycerol (Supporting Information Table S1) were thawed and inoculated (4%) into 10 mL GAM. The cultures were incubated at 37 °C overnight and for at least 24 h for slow-growing bacteria (*Akkermansia muciniphila*, *Alistipes indistinctus*, and *Veillonella parvula*). Before synthetic gut microbial-community reconstruction, each bacterium was pre-cultured again to obtain a stable growing culture. The optical densities of the pre-cultures were measured using a microplate reader as previously described. The optical densities of the bacterial pre-cultures were then adjusted to a final $OD_{600\ nm}$ of 0.1.

The pre-cultures were each diluted from $OD_{600\ nm}$ of 0.1 to $OD_{600\ nm}$ of 0.00125, 0.005, and 0.01 for fast- (*Actinobacteria* and *Firmicutes*), moderate- (*Bacteroides*), and slow-growing bacteria (*A. muciniphila*, *A. indistinctus*, and *V. parvula*) respectively in 15 mL of GAM. Bacteria diluted in either GAM were mixed to obtain a synthetic gut microbial community. Afterward, 3 mL of each bacterial solution was dispensed (n = 4/culture medium)

into 14 mL culture tubes containing mucin–agar gel. Emodin was added to a final concentration of 100 μmol L^{-1} and incubated at 37 °C for 36 h in an anaerobic chamber. Next, genomic DNA was extracted from bacteria on the mucin–agar and in the upper liquid. Before genomic DNA extraction, the mucin–agar solid gel was rinsed three times in sterile phosphate-buffered saline (PBS) to ensure that only bacteria capable of adhering to solid mucin–agar gel were retained.

Animal care and treatment with emodin

Animals are maintained under pathogen-free conditions in a facility at the Korea Institute of Science and Technology (KIST). The animal protocol was approved by the Institutional Animal Care and Use Committee of the KIST (approval number KIST-5088-2022-05-080). Five-week-old female CD45.1 mice, weighing 20–22 g, were bred at the KIST Gangneung Institute of Natural Products and randomly divided into a control group (vehicle only), low-emodin group (10 mg kg day^{-1}), and high-emodin group (50 mg kg day^{-1}) ($n \geq 6$ mice/group). For oral gavage, emodin was dissolved in 0.25% carboxymethyl cellulose solution on each day of treatment and fed to mice every day for a week under standard normal chow diet. The mice were housed in ventilated cages at 23 ± 0.5 °C in 40% humidity under a 12 h light–dark cycle with *ad libitum* access to feed and water during the entire experiment. All animals were acclimated for 7 days, and six animals were housed per cage, ensuring a similar average weight per cage. Mice were euthanized by isoflurane inhalation at the beginning of the light cycle after 16 h of food deprivation. The cecum and colon were collected in sterile tubes, immediately frozen in liquid nitrogen, and stored at −80 °C until use.

Microbial community analysis

Genomic DNA extraction was performed using the PowerFecal Pro-DNA Kit (Qiagen, Germantown, MD, USA), and the 16S rRNA gene was amplified using the Illumina-adapted universal primers, 341F and 805R, for the V3–V4 region. Polymerase chain reaction amplification was performed with an initial denaturation at 98 °C for 3 min, followed by 25 cycles of denaturation at 95 °C for 30 s, annealing at 55 °C for 30 s, and extension at 72 °C for 30 s, with a final extension at 72 °C for 5 min. The polymerase chain reaction products were purified and quantified using AMPure XT beads (Beckman Coulter Genomics, Danvers, MA, USA) and Qubit dsDNA High-Sensitivity Reagent (Invitrogen, Carlsbad, CA, USA) respectively. Sequencing was performed on the MiSeq platform using a MiSeq Reagent Kit v3 (600 cycle) (Illumina, San Diego, CA, USA). The demultiplexed sequences were assembled and quality-filtered using Quantitative Insights Into Microbial Ecology (QIIME) 2 software (version 2019.7).[21] A naive Bayes classifier was trained using the V3–V4 16S rRNA region, the 341/805R primer set, and the Greengenes 99% reference set (version 13.8) in QIIME 2 software. This trained feature classifier was then used for taxonomical assignments for each sequence, using the default settings of QIIME 2. Subsequent microbial analyses were conducted using MicrobiomeAnalyst.[22]

Isolation and intracellular staining of colonic Treg cells

Colon lamina propria (cLP) lymphocytes were isolated as described previously.[23] Briefly, the colons were collected and opened longitudinally, washed with PBS to remove all luminal contents, and shaken in Hank's balanced salt solution containing 5 mmol L^{-1} ethylenediaminetetraacetic acid (EDTA) for 20 min at 37 °C. After removing epithelial cells, muscle layers, and fat tissue using forceps, the cLP layers were cut into small pieces and incubated with RPMI 1640 containing 4% fetal bovine serum, 0.5 mg mL^{-1} collagenase D, 0.5 mg mL^{-1} dispase, and 40 μg mL^{-1} DNase I (all from Roche Diagnostics, Basel, Switzerland) for 1 h at 37 °C in a shaking water bath. Each digested tissue was washed with Hank's balanced salt solution containing 5 mmol L^{-1} EDTA, resuspended in 5 mL of 40% Percoll (GE Healthcare, Stockholm, Sweden), and overlaid on 80% Percoll in a 15 mL Falcon tube. Percoll-gradient separation was performed by centrifugation at 800 × *g* for 20 min at 25 °C. The cLP lymphocytes were collected from the interface of the Percoll gradient and suspended in ice-cold PBS. For Treg cell analysis, isolated lymphocytes were labeled using the LIVE/DEAD Fixable Dead Cell Stain Kit (Invitrogen) to exclude dead cells from the analysis. The cells were washed with staining buffer containing PBS, 2% fetal bovine serum, 2 mmol L^{-1} EDTA, and 0.09% NaN_3, and surface staining was performed with a PerCP–Cyanine 5.5-labeled anti-CD4 antibody (RM4-5; BD Biosciences, CA, USA). Intracellular staining of FOXP3, inducible co-stimulatory molecule (ICOS), Helios, retinoic acid-related orphan receptor (RORgt), and CD25-A488 was performed using an Alexa 647-labeled anti-FOXP3 antibody (FJK-16s, eBioscience, CA, USA), a fluorescein isothiocyanate labeled anti-COS antibody (C938.4A; BioLegend, CA, USA), a fluorescein isothiocyanate labeled anti-Helios antibody (22F6; BioLegend), an allophycocyanin-labeled anti-RORgt antibody (B56, BD Biosciences), an Alexa 488-labeled anti-CD25 antibody (22F6; BioLegend), and the FOXP3 Staining Buffer Set (eBioscience). After incubation for 4 h, the cells were washed in PBS, labeled using the LIVE/DEAD Fixable Dead Cell Stain Kit, and surface CD4 was stained with a phycoerythrin–cyanine 7 labeled anti-CD4 antibody. Cells were washed, fixed in Cytofix/Cytoperm, permeabilized with Perm/Wash buffer (BD Biosciences), and stained with the aforementioned antibodies. The antibody-stained cells were analyzed with an LSR Fortessa or FACS Aria III flow cytometer (BD Biosciences), and the resulting data were analyzed using FlowJo software (Tree Star Inc. Ashland, OR, USA).

Statistical analysis

GraphPad Prism software (version 8.4.0; GraphPad Software, La Jolla, CA, USA) was used to perform statistical analysis of the data for all groups. Each group was compared using Student's *t*-test, the Mann–Whitney test, and one-way or two-way analysis of variance corrected for multiple comparisons with a Sidak test, and differences were declared significant at $P < 0.05$. In addition, MicrobiomeAnalyst was used for processing microbial data.[22] First, non-metric multidimensional scaling plots were generated by performing Bray–Curtis dissimilarity analysis to visually represent the compositional differences in the microbiota among groups. The Sparse Correlations for Compositional data (SparCC) algorithm method was then used to select subsets of taxa (genus level) that were highly discriminative for distinct communities in the emodin-treated and control groups.[24] Finally, to select subsets of taxa to species level that were differentially abundant between groups, linear discriminant analysis effect size was applied under the condition $\alpha = 0.05$ with linear discriminant analysis score of ≥2.[25]

RESULTS AND DISCUSSION

Emodin modulated bacterial growth in monocultures

There is considerable interest in using dietary approaches, including phytochemicals, to modulate the GM composition and improve health. In this study, bacterial growth, relative microbial

abundances, and Treg immune-cell staining were evaluated after treating GM samples with anthraquinones such as emodin. First, gut bacterial isolates were treated with emodin in GAM at a final concentration of 100 μmol L^{-1}, which is close to or equal to the concentration used in another *in vitro* study.[4] Therefore, we purposively selected a concentration of 100 μmol L^{-1} for this study. All isolates grew well in GAM except for *Faecalibacterium prausnitzii*, which was suggestive of a medium limitation for the *in vitro* culture experiments. This limitation could reflect the previous observation that GM species have different nutritional requirements, which may affect the growth of *F. prausnitzii* in GAM.[20] Nevertheless, a correlation between the response to these anthraquinone compounds and the bacterial-growth characteristics was observed, as revealed by changes in the growth of various bacterial strains under the influence of these compounds (Fig. 1).

Compared with other anthraquinones used in this study, emodin had a relatively strong inhibitory effect on the growth of human gut bacteria isolates, especially those in the phylum *Bacteroidetes*. Previous data have correlated *Bacteroidetes* spp. with the development of ulcerative colitis.[26] Interestingly, emodin markedly inhibited the growth of *Bacteroidetes*, whereas health-associated commensal bacteria such as *Akkermansia* and *Roseburia*[27] were not adversely affected by emodin treatment (Fig. 1), indicating the strong GM modulation effect by emodin. However, emodin was not active against *Escherichia coli*, which is also regarded as a cause of gut inflammation.[28] This finding agrees with a previous report showing that emodin was inactive against two Gram-negative bacteria, namely *Klebsiella* and *Escherichia*.[29]

Emodin changed the microbial composition of the synthetic gut ecosystem

To assess the GM-modulatory effects of emodin, synthetic gut microbial communities were transferred to GAM in a simulated mucosal environment and treated with emodin at 100 μmol L^{-1}, followed by high-throughput bacterial 16S rRNA gene sequencing. Both simulated mucosal and luminal microbiotas were examined after incubating them for 36 h at 37 °C following emodin treatment. After merging, filtration, and taxonomic annotation of the raw sequencing reads obtained for the synthetic gut microbial communities, the relative abundances of the operational taxonomic units in each sample were analyzed further. First, it was observed that bacteria distinctively separated into mucosal-related microbiota and luminal microbiota, with each group (mucosal or luminal) again clustering into distinct groups based on emodin treatment (Fig. 2(A)). Known mucosal residents, such as *Akkermansia*, *Clostridium*, *Faecalibacterium*, and *Roseburia*, efficiently colonized the simulated mucosal environment, whereas known luminal bacteria, like *Alistipes*, *Bacteroides*, *Veillonella*, and *Prevotella*, colonized the luminal part (Fig. 2(B)).

These results of the mucosal microbiota simulation indicate the effectiveness of the gut-mucosal environment simulation in this study and corroborate previous *in vitro*[16] and *in vivo*[30] data revealing differences in mucosal and luminal microbiota. Emodin treatment in the synthetic gut ecosystem decreased relative abundances of two major enterotypes, namely *Bacteroides* and *Prevotella* (Fig. 3). These findings corroborate our monoculture results, where emodin significantly inhibited the growth of *Bacteroides* and *Prevotella* (Fig. 1). Taken together, these data show that emodin consistently inhibited *Bacteroides* and *Prevotella* in both monoculture and co-culture. *Bacteroides* and *Prevotella* bacteria have been implicated in the development and progression of gut inflammation, as previously mentioned in this study.

Although *Blautia*, *Clostridium*, *Faecalibacterium*, and *Roseburia* were enriched in the simulated mucosal layers (Fig. 2(B)), emodin specifically increased the relative abundance of *Faecalibacterium* and *Roseburia* (Fig. 3(A)). A significant reduction in the abundance of *Roseburia* has been observed in patients with ulcerative colitis[31] and inflammatory bowel diseases (IBDs).[32] In particular, *Roseburia* can exert anti-inflammatory actions[33] together with *Faecalibacterium* to protect the intestines by producing important short-chain fatty acids such as butyrate.[34] Our observation that emodin promoted the growth and relative abundance of *Roseburia* and *Faecalibacterium*, decreasing relative abundances of enterotypes

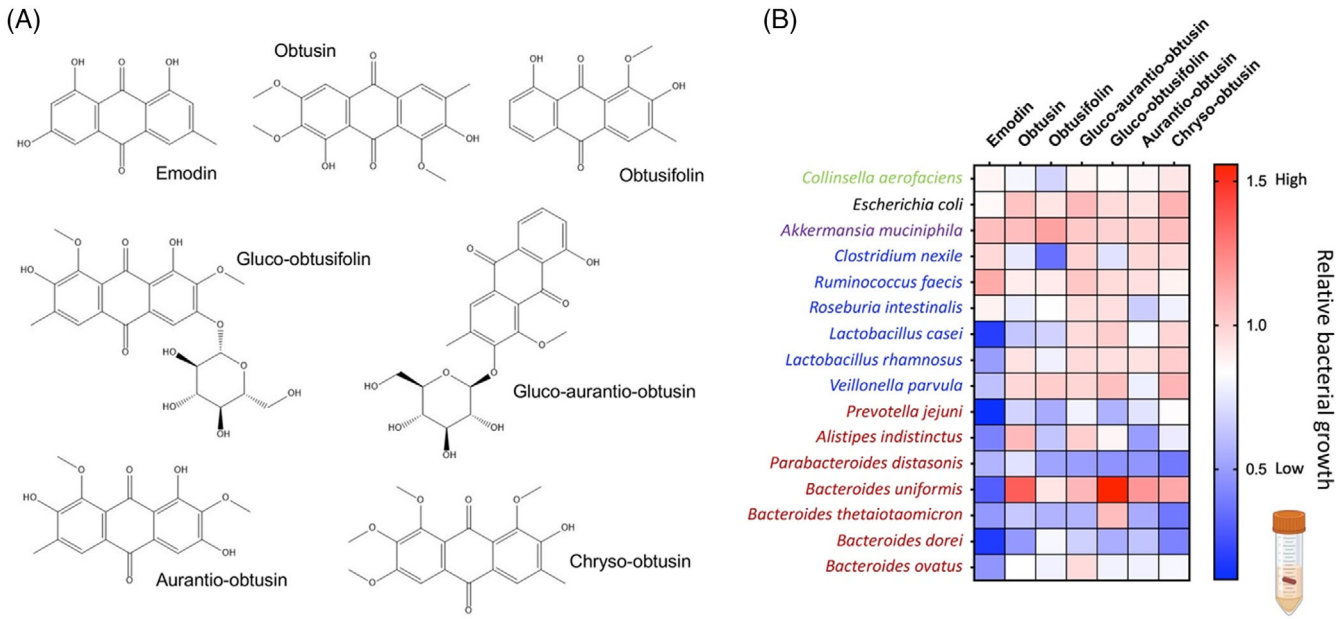

Figure 1. Effects of emodin on single-bacteria cultures, as determined by heatmap analysis. (A) Emodin and other six anthraquinones chemicals were added to the culture of each bacterium at 100 μmol L^{-1}, after which (B) growth was measured at $OD_{600\ nm}$. The text colors indicate bacteria in the same phyla, as follows: green (*Actinobacteria*), black (*Proteobacteria*), purple (*Verrumicrobia*), blue (*Firmicutes*), and red (*Bacteroidetes*).

Journal of The Science of Food and Agriculture published by John Wiley & Sons Ltd on behalf of Society of Chemical Industry.

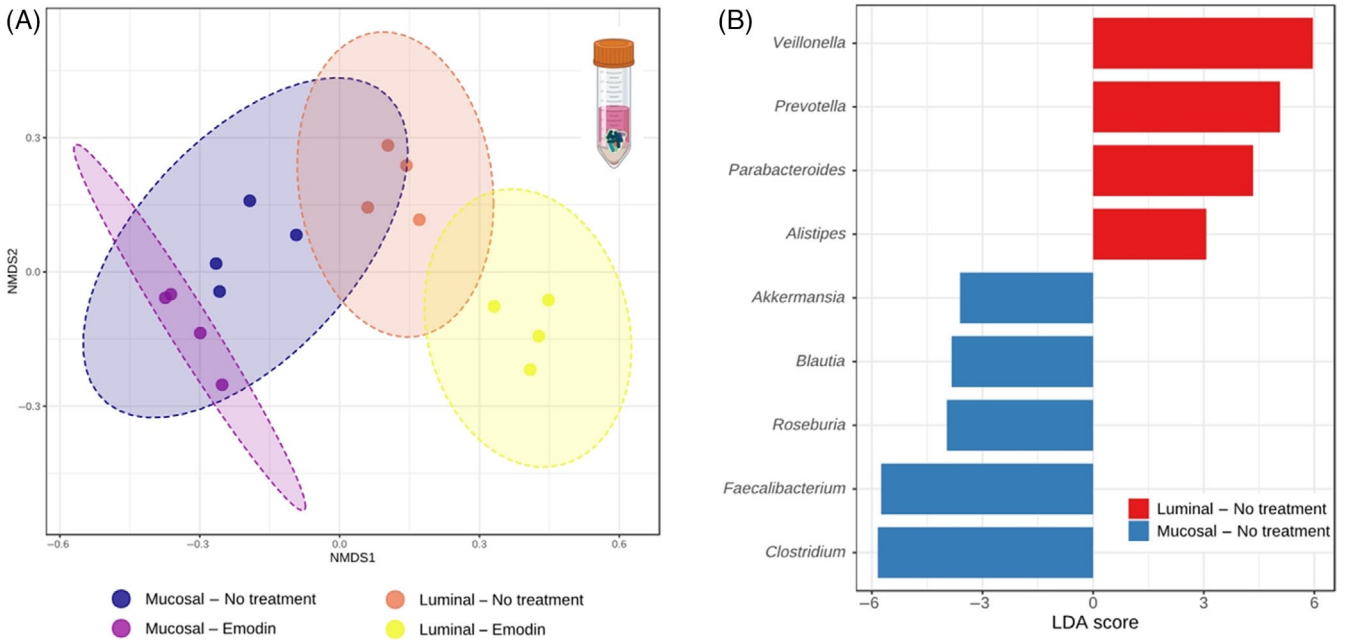

Figure 2. Effects of emodin on synthetic gut-microbial communities. The mucosal environment was simulated by adding solid mucin–agar gel to the bottom of culture tubes. (A) A β-diversity non-metric multidimensional scaling plot of microbial community where bacteria distinctively clustered based on mucosal environment simulation and emodin treatment. (B) Linear discriminant analysis (LDA) showing specific microbiota to efficiently colonize the mucosal solid part, whereas others dominated in the luminal liquid part.

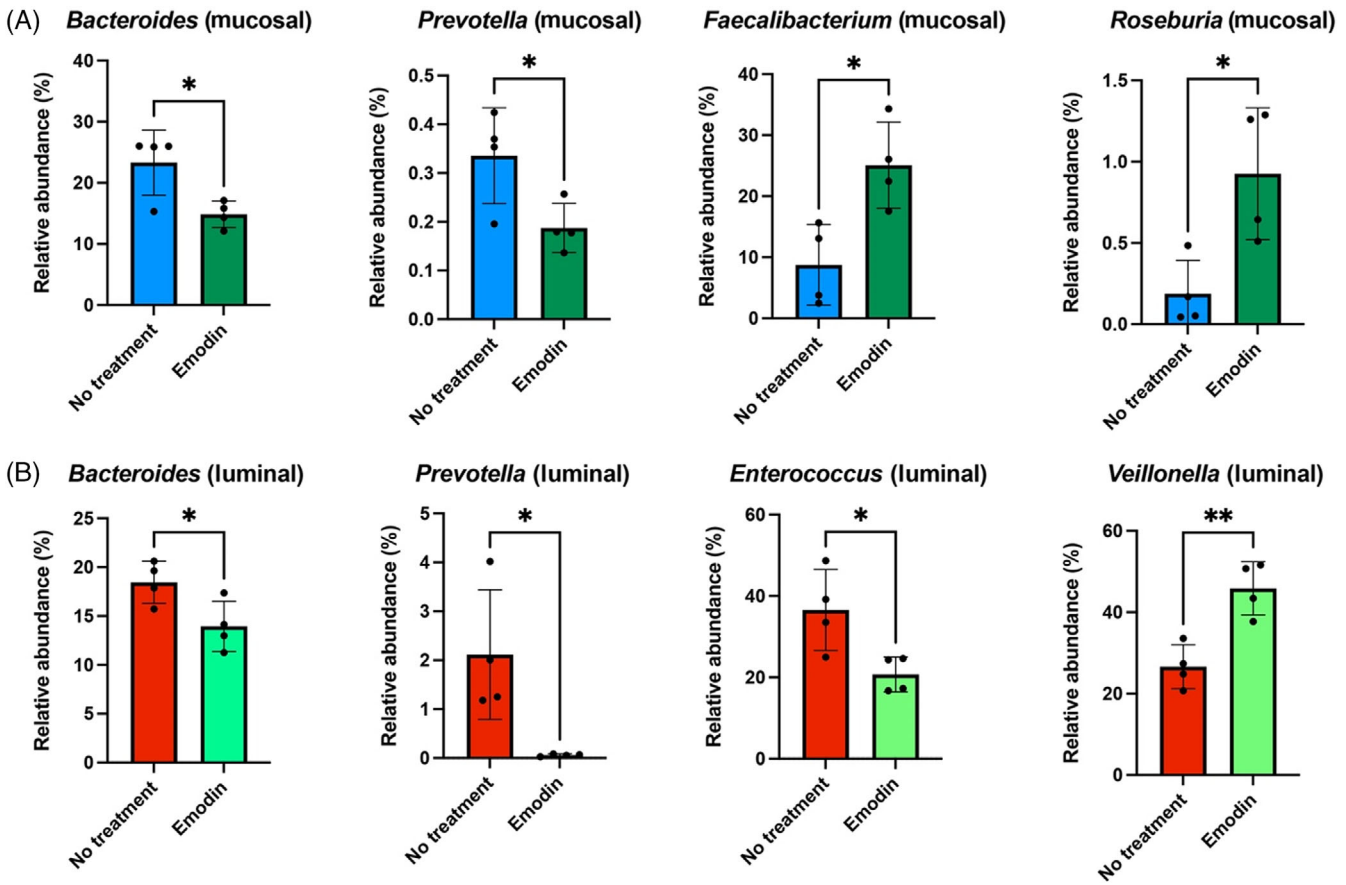

Figure 3. Bar graphs showing the effects of emodin on relative bacterial abundance in the (A) mucosal and (B) luminal part through a synthetic gut microbial ecosystem. Emodin significantly increased the relative abundance of beneficial microbes (*Faecalibacterium* and *Roseburia*) and inhibited inflammation-related microbes (*Bacteroides* and *Prevotella*) and opportunistic gut pathogen (*Enterococcus*). Statistical significance was determined using Student's *t*-test ($n = 4$/group; $P < 0.05$).

associated with gut inflammation while regulating potential gut pathogens such as *Enterococcus* (Fig. 3), might suggest that emodin supplementation in food could contribute to an overall improvement in gut health.

We also observed that *Faecalibacterium* could not grow as a monoculture in GAM but that it was abundantly detected in co-culture. Regarding monocultures, previous results indicated that *Faecalibacterium* growth was strongly stimulated in the presence of acetate[35] or that it could grow in GAM supplemented with bovine rumen, cellobiose, and inulin.[36] These findings indicate that this bacterium benefits from interaction with other bacteria included in the synthetic gut microbial consortium. The results of another study showed that co-cultured *Faecalibacterium* benefit from cross-feeding of acetate derived from *Bacteroides*.[37] These data highlight the strength of synthetic gut microbial communities during GM cultivation and subsequent treatment with chemicals.

The *in vitro* effects of emodin replicated *in vivo*

In this study, we also sought to understand whether synthetic gut microbial communities could be used to demonstrate the impact of emodin on the mouse GM. After simulating the gut-microbial ecosystem and applying emodin treatment, we investigated whether the results could be replicated *in vivo (*Fig. 4).

The non-metric, multidimensional scaling β-diversity index indicated the different clusters of the GM community among the control, low-emodin (10 mg.kg^{-1}), and high-emodin (50 mg kg^{-1}) groups (Fig. 4(A)). The high-emodin group was distinguished from the control and low-emodin group, indicating that high emodin

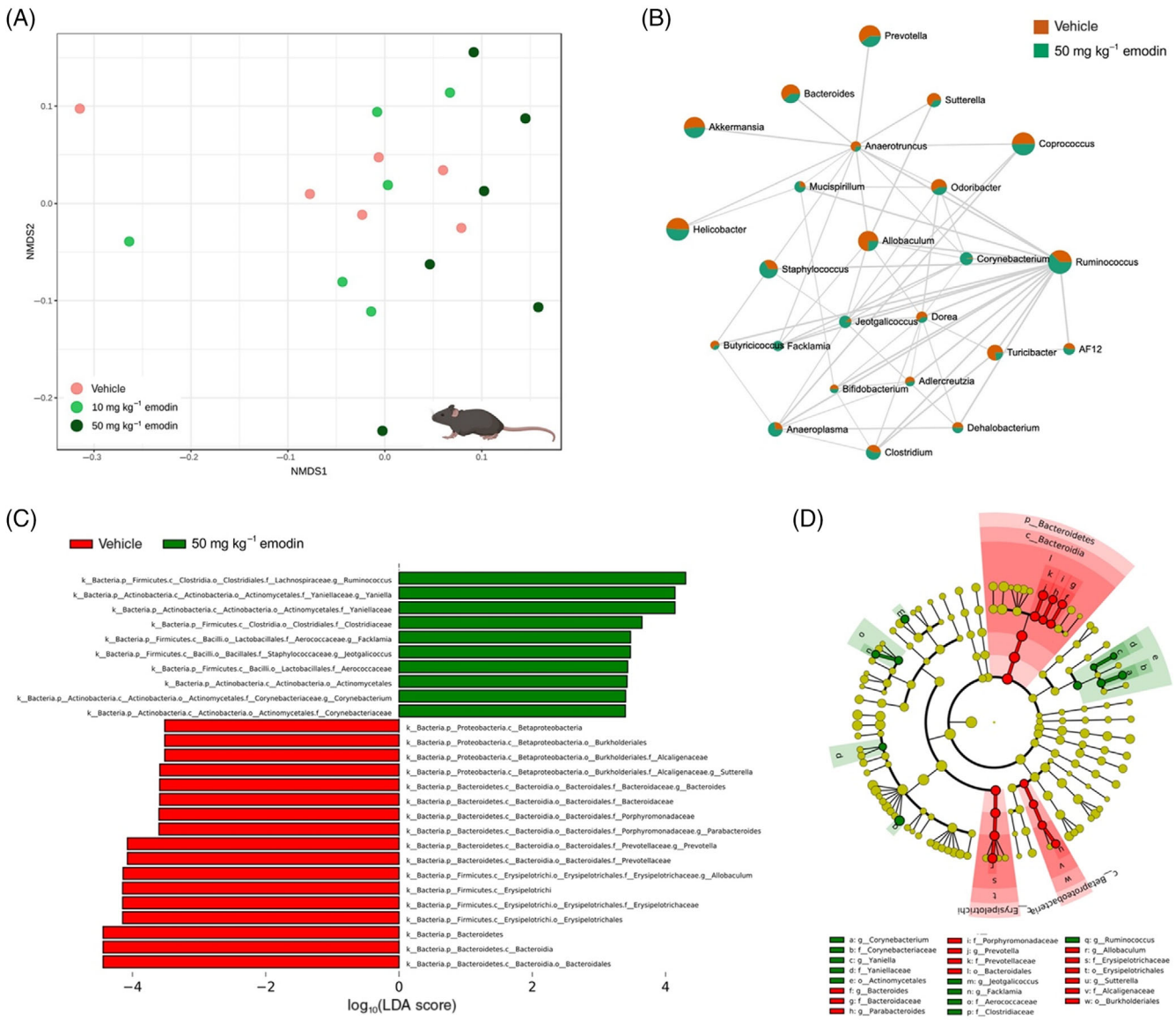

Figure 4. (A) Mice cecum microbial-community profiling. β-diversity index; ordination method: NMDS; distance method: Bray–Curtis distance matrix; statistical method: permutational multivariate analysis of variance. Each dot represents a mouse, $n \geq 6$/group. (B) SparCC network plot of bacterial interactions following emodin treatment. Nodes represent detected phylotypes (OTU clustered at 97% similarity) and shows fraction of increase/decrease where emodin increased *Clostridium* and *Ruminococcus* and decreased *Bacteroides* and *Prevotella*. Linear discriminant analysis (LDA) effect size analysis. (C) Bar chart indicating the log-transformed LDA scores between groups and (D) cladogram indicating the phylogenetic relationships of bacteria taxa between emodin and control group ($n \geq 6$/group).

Journal of The Science of Food and Agriculture published by John Wiley & Sons Ltd on behalf of Society of Chemical Industry.

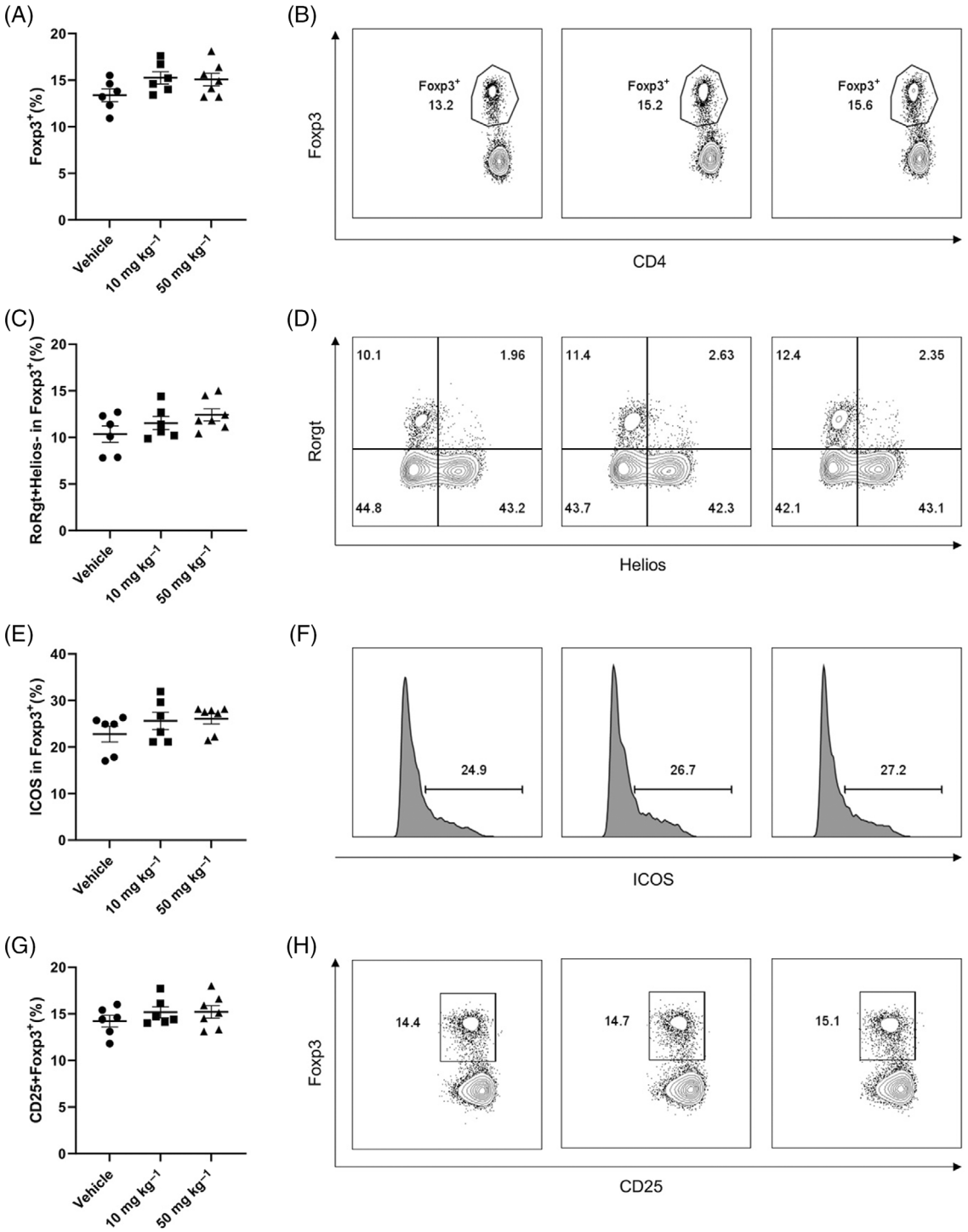

Figure 5. Increased cellular expression of forkhead box P3 transcription factor (Foxp3), Helios, retinoic acid-related orphan receptor (RORgt), and inducible co-stimulatory molecule (ICOS) in mice treated with emodin. Colon lamina propria (cLP) lymphocytes were isolated and the expression levels of Foxp3, Helios, RORgt, and ICOS were analyzed after intracellular staining. (A, C, E, G) Representative dot-plots of the percentages of cells expressing Foxp3, Helios, RORgt, and ICOS among the CD4 cell population in individual mice. (B, D, F, H) Fluorescence-activated cell sorting plots of CD4, Foxp3, Helios, and ICOS expression in immune cells in the cLP. The numbers in the quadrants represent cell frequencies, and the circles in the graph plots represent individual mice corresponding to each parameter ($n \geq 6$ mice).

induced microbial-population differences, when compared with those observed after low-emodin treatment.

The SparCC algorithm and linear discriminant analysis effect size were performed to determine the effects of emodin *in vivo* (Fig. 4(B)–(D)). Comparing the results shown in Fig. 4(B)–(D) with the results obtained with synthetic gut-microbial communities (Fig. 2) revealed a resemblance between *Bacteroides* and *Prevotella*, where emodin treatment decreased their relative abundances in both cases (*in vitro* synthetic gut microbial ecosystem and *in vivo*). Interestingly, major gut enterotypes (*Bacteroides* and

Prevotella) that are related to gut inflammation were similarly affected by emodin in monocultures, co-cultures of synthetic gut microbial communities, and *in vivo* (Figs 1–4). Nonetheless, our *in vivo* results agree with those of a previous study that indicated emodin decreased the abundances of *Bacteroides* and *Prevotella in vivo*.[18] These findings further indicate that the luminal microbiota of the synthetic gut-microbial ecosystem model matched the *in vivo* results.

In contrast, beneficial butyrate-producing mucosal microbiota like *Akkermansia*, *Faecalibacterium*, and *Roseburia* observed with our synthetic gut-microbial ecosystem model were not robustly detected *in vivo*, apart from *Clostridium* (Fig. 4(B)–(D)). Even though *Faecalibacterium* and *Roseburia* were not increased by emodin *in vivo*, emodin increased the relative abundance of *Clostridium* and *Ruminococcus*, which are beneficial butyrate-producing gut bacteria (Fig. 4(B), (C)).[38] Failure to detect these mucosal bacteria *in vivo* may not be surprising considering that the GM mainly comprises the luminal microbiota, with mucosal microbiota being less common in most studies.[39] Furthermore, a mucosal microbiota such as *Roseburia* could not have maximally colonized the mice used in this study due to variables such as breeding, cage environment, sex, and age, which were associated with GM variations, hence making them undetectable.[40] The values of the α-diversity indices (Chao, Simpson, and Shannon) used to describe the ecological diversity of the gut microbiome were not significant among the three study groups (data not shown). These findings could be attributed to the fact that only normal mice and mice treated with emodin for 7 days were used in this study, as opposed to other murine disease models; therefore, the α-diversity values of the control group were sufficiently high.

Emodin altered Treg intestinal immunity and associated anti-inflammatory factors *in vivo*

$Foxp3^+$ $CD4^+$ cells are the most common Treg immune cells in the intestine. The GM, especially *Clostridium* spp., impacts the growth and function of these cells.[41] Previous data showed that short-chain fatty acids, primarily butyrate (generated by clostridia strains during the fermentation of starch and other dietary fibers) contributed to colonic Treg generation.[42] These cells can selectively detect inflammatory signals, which activate them and increase their suppressive power to combat inflammation and inflammation-related tissue damage.[43] In this study, emodin tended to increase Treg immunity and expression of the anti-inflammatory transcription factor $Foxp3^+$, and regulated the expression levels of $Foxp3^+$-associated elements, namely Helios, RORgt, and ICOS (Fig. 5).

Although the effect is not significant, the immune analysis from *in vivo* samples showed an increasing trend of Treg, indicating that the change in microbial community may link to the host intestinal immune regulation. Consistent with these findings, emodin increased the relative *in vivo* abundance of *Clostridium* and *Ruminococcus*, which are butyrate producers (Fig. 4(B), (C)).[38] Emodin also increased the abundances of other clostridia, such as *Clostridium* (Fig. 1), *Roseburia* (Figs 1 and 3) and *Faecalibacterium* (Fig. 3). On a translational note, the abundances of colonic butyrate-producing bacteria were found to be decreased in human patients with IBD.[44] This outcome could lead to a decrease in the anti-inflammatory factor, in turn leading to the onset and further development of IBD. Interestingly, in this study, emodin increased the levels of butyrate-producing bacteria and related anti-inflammatory factors and reduced the relative abundances of bacteria associated with IBD development. These results suggest that emodin can be used to control gut inflammation and IBD.

In this study, emodin induced similar GM responses *in vitro* and *in vivo*, particularly for major enterotypes *Bacteroides* and *Prevotella*. *In vivo* models are labor intensive, costly, and require ethical approval.[45] Hence, *in vitro* models are becoming more common in GM studies. However, some *in vitro* models are complex and can simulate physiological functions, but access to such devices is often limited and expensive.[46] In contrast, the cultivation of synthetic gut-microbial communities in batch bioreactors designed to represent mucosal and luminal environments is rapid and cost effective, without the need to consider ethical issues. Nonetheless, the microbiotas of animals often change, and these communities can help improve the reproducibility of GM studies.[47]

CONCLUSION

This study suggests the possibility of modulating GM and improve health by emodin. It was observed that emodin induced similar GM changes in both synthetic gut microbiome model and *in vivo* mice experiment. Emodin stimulated the growth of beneficial bacteria but inhibited major gut enterotypes (*Bacteroides* and *Prevotella*). In addition, colonic Treg cells analysis showed that emodin stimulated Treg immune responses *in vivo*. This study has demonstrated that single bacteria culture, a synthetic gut ecosystem, and an *in vivo* mice experiment can be appropriately used for diverse microbiome research in that they each have their own characteristics and show consistent results for major microbiome changes. Further research is warranted to elucidate the in-depth relevant mechanism on how emodin modulates GM.

ABBREVIATIONS USED

ATCC	American Type Culture Collection
CD4	cluster of differentiation 4
cLP	colon lamina propria
CMC	carboxymethyl cellulose
DM	defined medium
DMSO	dimethyl sulfoxide
EDTA	ethylenediaminetetraacetic acid
FBS	fetal bovine serum
FITC	fluorescein isothiocyanate
Foxp3	forkhead box P3 transcription factor
GAM	Gifu anaerobic medium
GM	gut microbiota
HBSS	Hank's balanced salt solution
HCl	hydrochloric acid
IBD	inflammatory bowel disease
ICOS	inducible co-stimulatory molecule
KCTC	Korean Collection for Type Cultures
NMDS	non-metric multidimensional scaling
OD	optical density
PBS	phosphate-buffered saline
PCR	polymerase chain reaction
QIIME	Quantitative Insights Into Microbial Ecology
RORgt	retinoic acid-related orphan receptor
SCFA	short-chain fatty acid
Treg	regulatory T cell

FUNDING SOURCES

This work was supported by a National Research Foundation of Korea (NRF) grant funded by the Korean government (MSIT)

(grant number 2021R1C1C1007945) and an Intramural Grant Scholarship and Innovation Fund (grant number PASET-RSIF). We acknowledge the SACIDS Foundation for One Health at the Sokoine University of Agriculture in Tanzania for hosting this fellowship.

CONFLICTS OF INTEREST

The authors declare no competing financial interest.

SUPPORTING INFORMATION

Supporting information may be found in the online version of this article.

REFERENCES

1 Monks TJ, Hanzlik RP, Cohen GM, Ross D and Graham DG, Quinone chemistry and toxicity. *Toxicol Appl Pharmacol* **112**:2–16 (1992).
2 Dong X, Fu J, Yin X, Cao S, Li X, Lin L *et al.*, Emodin: a review of its pharmacology, toxicity and pharmacokinetics. *Phytother Res* **30**: 1207–1218 (2016).
3 Shia CS, Hou YC, Tsai SY, Huieh PH, Leu YL and Chao PD, Differences in pharmacokinetics and *ex vivo* antioxidant activity following intravenous and oral administrations of emodin to rats. *J Pharm Sci* **99**: 2185–2195 (2010).
4 Liu Z, de Bruijn WJC, Bruins ME and Vincken JP, Reciprocal interactions between epigallocatechin-3-gallate (EGCG) and human gut microbiota *in vitro*. *J Agric Food Chem* **68**:9804–9815 (2020).
5 Jandhyala SM, Talukdar R, Subramanyam C, Vuyyuru H, Sasikala M and Nageshwar Reddy D, Role of the normal gut microbiota. *World J Gastroenterol* **21**:8787–8803 (2015).
6 Shaw KA, Bertha M, Hofmekler T, Chopra P, Vatanen T, Srivatsa A *et al.*, Dysbiosis, inflammation, and response to treatment: a longitudinal study of pediatric subjects with newly diagnosed inflammatory bowel disease. *Genome Med* **8**:75 (2016).
7 Verma R, Lee C, Jeun EJ, Yi J, Kim KS, Ghosh A *et al.*, Cell surface polysaccharides of *Bifidobacterium bifidum* induce the generation of Foxp3$^+$ regulatory T cells. *Sci Immunol* **3**:eaat6975 (2018).
8 Furusawa Y, Obata Y, Fukuda S, Endo TA, Nakato G, Takahashi D *et al.*, Commensal microbe-derived butyrate induces the differentiation of colonic regulatory T cells. *Nature* **504**:446–450 (2013).
9 Wu H-J and Wu E, The role of gut microbiota in immune homeostasis and autoimmunity. *Gut Microbes* **3**:4–14 (2012).
10 Fontenot JD, Rasmussen JP, Williams LM, Dooley JL, Farr AG and Rudensky AY, Regulatory T cell lineage specification by the forkhead transcription factor Foxp3. *Immunity* **22**:329–341 (2005).
11 Pandey KR, Naik SR and Vakil BV, Probiotics, prebiotics and synbiotics – a review. *J Food Sci Technol* **52**:7577–7587 (2015).
12 Duda-Chodak A, The inhibitory effect of polyphenols on human gut microbiota. *J Physiol Pharmacol* **63**:497–503 (2012).
13 Park JM, Shin Y, Kim SH, Jin M and Choi JJ, Dietary epigallocatechin-3-gallate alters the gut microbiota of obese diabetic db/db mice: *Lactobacillus* is a putative target. *J Med Food* **23**:1033–1042 (2020).
14 Lozupone CA, Stombaugh JI, Gordon JI, Jansson JK and Knight R, Diversity, stability and resilience of the human gut microbiota. *Nature* **489**:220–230 (2012).
15 Rajilić-Stojanović M and de Vos WM, The first 1000 cultured species of the human gastrointestinal microbiota. *FEMS Microbiol Rev* **38**: 996–1047 (2014).
16 Mabwi HA, Hitayezu E, Mauliasari IR, Mwaikono KS, Yoon HS, Komba EVG *et al.*, Simulation of the mucosal environment in the re-construction of the synthetic gut microbial ecosystem. *J Microbiol Methods* **191**:106351 (2021).
17 Sun J, Luo JW, Yao WJ, Luo XT, Su CL and Wei YH, Effect of emodin on gut microbiota of rats with acute kidney failure. *Zhongguo Zhong Yao Za Zhi* **44**:758–764 (2019).
18 Ye ZP, Wu KR, Jin F, Xu T, Li N and Huang J, Effect of emodin on intestinal flora in the treatment of iodine-induced thyroiditis in NOD mice. *Int J Clin Exp Med* **13**:1493–1500 (2020).
19 Forster SC, Kumar N, Anonye BO, Almeida A, Viciani E, Stares MD *et al.*, A human gut bacterial genome and culture collection for improved metagenomic analyses. *Nat Biotechnol* **37**:186–192 (2019).
20 Tramontano M, Andrejev S, Pruteanu M, Klunemann M, Kuhn M, Galardini M *et al.*, Nutritional preferences of human gut bacteria reveal their metabolic idiosyncrasies. *Nat Microbiol* **3**:514–522 (2018).
21 Bolyen E, Rideout JR, Dillon MR, Bokulich NA, Abnet CC, Al-Ghalith GA *et al.*, Reproducible, interactive, scalable and extensible microbiome data science using QIIME 2. *Nat Biotechnol* **37**:852–857 (2019).
22 Dhariwal A, Chong J, Habib S, King IL, Agellon LB and Xia J, MicrobiomeAnalyst: a web-based tool for comprehensive statistical, visual and meta-analysis of microbiome data. *Nucleic Acids Res* **45**:W180–W188 (2017).
23 Basu R, Whitley SK, Bhaumik S, Zindl CL, Schoeb TR, Benveniste EN *et al.*, IL-1 signaling modulates activation of STAT transcription factors to antagonize retinoic acid signaling and control the TH17 cell–iTreg cell balance. *Nat Immunol* **16**:286–295 (2015).
24 Friedman J and Alm EJ, Inferring correlation networks from genomic survey data. *PLoS Comput Biol* **8**:e1002687 (2012).
25 Segata N, Izard J, Waldron L, Gevers D, Miropolsky L, Garrett WS *et al.*, Metagenomic biomarker discovery and explanation. *Genome Biol* **12**:R60 (2011).
26 Lucke K, Miehlke S, Jacobs E and Schuppler M, Prevalence of *Bacteroides* and *Prevotella* spp. in ulcerative colitis. *J Med Microbiol* **55**: 617–624 (2006).
27 Hiippala K, Jouhten H, Ronkainen A, Hartikainen A, Kainulainen V, Jalanka J *et al.*, The potential of gut commensals in reinforcing intestinal barrier function and alleviating inflammation. *Nutrients* **10**:988 (2018).
28 Rhodes JM, The role of *Escherichia coli* in inflammatory bowel disease. *Gut* **56**:610–612 (2007).
29 Chukwujekwu JC, Coombes PH, Mulholland DA and van Staden J, Emodin, an antibacterial anthraquinone from the roots of *Cassia occidentalis*. *South Afr J Bot* **72**:295–297 (2006).
30 Nava GM, Friedrichsen HJ and Stappenbeck TS, Spatial organization of intestinal microbiota in the mouse ascending colon. *ISME J* **5**:627–638 (2011).
31 Machiels K, Joossens M, Sabino J, De Preter V, Arijs I, Eeckhaut V *et al.*, A decrease of the butyrate-producing species *Roseburia hominis* and *Faecalibacterium prausnitzii* defines dysbiosis in patients with ulcerative colitis. *Gut* **63**:1275–1283 (2014).
32 Kumari R, Ahuja V and Paul J, Fluctuations in butyrate-producing bacteria in ulcerative colitis patients of north India. *World J Gastroenterol* **19**:3404–3414 (2013).
33 Shen Z, Zhu C, Quan Y, Yang J, Yuan W, Yang Z *et al.*, Insights into *Roseburia intestinalis* which alleviates experimental colitis pathology by inducing anti-inflammatory responses. *J Gastroenterol Hepatol* **33**: 1751–1760 (2018).
34 Kostic AD, Chun E, Meyerson M and Garrett WS, Microbes and inflammation in colorectal cancer. *Cancer Immunol Res* **1**:150–157 (2013).
35 Duncan SH, Hold GL, Harmsen HJM, Stewart CS and Flint HJ, Growth requirements and fermentation products of *Fusobacterium prausnitzii*, and a proposal to reclassify it as *Faecalibacterium prausnitzii* gen. nov., comb. nov. *Int J Syst Evol Microbiol* **52**:2141–2146 (2002).
36 Bellais S, Nehlich M, Ania M, Duquenoy A, Mazier W, van den Engh G *et al.*, Species-targeted sorting and cultivation of commensal bacteria from the gut microbiome using flow cytometry under anaerobic conditions. *Microbiome* **10**:24 (2022).
37 Murakami R, Hashikura N, Yoshida K, Xiao JZ and Odamaki T, Growth-promoting effect of alginate on *Faecalibacterium prausnitzii* through cross-feeding with *Bacteroides*. *Food Res Int* **144**:110326 (2021).
38 Takahashi K, Nishida A, Fujimoto T, Fujii M, Shioya M, Imaeda H *et al.*, Reduced abundance of butyrate-producing bacteria species in the fecal microbial community in Crohn's disease. *Digestion* **93**:59–65 (2016).
39 Wu M, Li P, Li J, An Y, Wang M and Zhong G, The differences between luminal microbiota and mucosal microbiota in mice. *J Microbiol Biotechnol* **30**:287–295 (2020).
40 Miyoshi J, Leone V, Nobutani K, Musch MW, Martinez-Guryn K, Wang Y *et al.*, Minimizing confounders and increasing data quality in murine models for studies of the gut microbiome. *PeerJ* **6**:e5166 (2018).
41 Nagano Y, Itoh K and Honda K, The induction of Treg cells by gut-indigenous *Clostridium*. *Curr Opin Immunol* **24**:392–397 (2012).
42 Sharma A and Rudra D, Emerging functions of regulatory T cells in tissue homeostasis. *Front Immunol* **9**:883 (2018).
43 van der Veeken J, Gonzalez AJ, Cho H, Arvey A, Hemmers S, Leslie CS *et al.*, Memory of inflammation in regulatory T cells. *Cell* **166**:977–990 (2016).
44 Frank DN, St Amand AL, Feldman RA, Boedeker EC, Harpaz N and Pace NR, Molecular–phylogenetic characterization of microbial community imbalances in human inflammatory bowel diseases. *Proc Natl Acad Sci U S A* **104**:13780–13785 (2007).

45 Bohn T, Carriere F, Day L, Deglaire A, Egger L, Freitas D *et al.*, Correlation between *in vitro* and *in vivo* data on food digestion. What can we predict with static *in vitro* digestion models? *Crit Rev Food Sci Nutr* **58**:2239–2261 (2018).
46 Mulet-Cabero AI, Egger L, Portmann R, Menard O, Marze S, Minekus M *et al.*, A standardised semi-dynamic *in vitro* digestion method suitable for food – an international consensus. *Food Funct* **11**: 1702–1720 (2020).
47 Rausch P, Basic M, Batra A, Bischoff SC, Blaut M, Clavel T *et al.*, Analysis of factors contributing to variation in the C57BL/6J fecal microbiota across German animal facilities. *Int J Med Microbiol* **306**:343–355 (2016).

